Fermi National Accelerator Laboratory

FN-460

Coupled Bunch Instability in Fermilab Booster and Possible Cures - Longitudinal Phase-Space Simulation*

S. Stahl and S.A. Bogacz
Fermi National Accelerator Laboratory
P.O. Box 500, Batavia, Illinois 60510

September 1987

*Submitted to Phys. Rev. D.

Operated by Universities Research Association Inc. under contract with the United States Department of Energy

FN - 460

COUPLED BUNCH INSTABILITY IN FERMILAB BOOSTER AND POSSIBLE CURES - LONGITUDINAL PHASE-SPACE SIMULATION

S. Stahl and S.A. Bogacz

Accelerator Theory Department, Fermi National Accelerator Laboratory,
P.O. Box 500, Batavia, IL 60510, USA

September 1987

PACS 29.20. - c

ABSTRACT

Coupled bunch instabilities in a circular machine are effectively simulated using a longitudinal phase-space tracking code (ESME). Two damping schemes based on intra-bunch (Landau cavity) and bunch-to-bunch synchrotron tune spread are also examined. Some comparison of the tune spread induced via these schemes (as a measure of introduced Landau damping) is done in both cases. Finally, a simulation of active damping of the coupled bunch instability through radial position feedback is explored as another possible cure.

INTRODUCTION

In this article we employ a longitudinal phase-space tracking code (ESME)[1] as an effective tool to simulate specific coupled bunch modes arising in a circular accelerator. We also use it to study the effect of possible cures aimed at eliminating or limiting growth of these instabilities. Most of our discussion is confined to three basic damping schemes: induced intra-bunch tune spread due to a so-called Landau cavitiy, bunch-to-bunch tune spread generated by a secondary voltage source of lower harmonic number and active damping through radial position feedback. In the first two cases stability against the growing coupled bunch modes is gained through the introduced incoherency among the particles in longitudinal phace-space. The third scheme involves fixed energy kicks applied to each bunch on a turn-by-turn basis through a feedback loop.

1. LONGITUDINAL PHASE-SPACE TRACKING WITH WAKE FIELDS

Briefly summarized, the tracking procedure used in ESME consists of turn-by-turn iteration of a pair of Hamilton-like difference equations describing synchrotron oscillation in θ-ε phase-space ($0 \le \theta \le 2\pi$ for the whole ring and $\varepsilon = E - E_0$, where E_0 is the synchronous particle energy). In order to include the effect of the beam environment one can consider the additional potential due to the wake field generated by the beam as it passes through the vacuum pipe. Knowing the particle distribution in the azimuthal direction, $\rho(\theta)$, and the revolution frequency, ω_0, after each turn, one can construct a wake field induced voltage as follows[2]

$$V_i(\theta) = e\omega_0 \sum_n \rho_n Z(n\omega_0) e^{in\theta} , \qquad (1)$$

where ρ_n represents the discrete Fourier spectrum of the beam and $Z(\omega)$ is a longitudinal coupling impedance. The numerical procedure involved in evaluating the above expression, Eq. (1), necessarily employs a discretization of the θ-direction. Some caution is required in this process of binning, due to the finite statistics inherent in such a simulation.

2. PARASITIC RESONANCES - MODE CROSSING

The longitudinal coupling impedance experienced by the beam in the Fermilab Booster (based upon measurements by J. Crisp[3]) consists of a broad-band part associated with the magnet laminations and a number of sharp parasitic resonances of the r.f. cavities. Each resonance can be modelled by the harmonic resonator of the impedance given by the standard expression:

$$Z(\omega) = \frac{R}{1 + iQ(\omega/\omega_c - \omega_c/\omega)} \ . \qquad (2)$$

Here R is the shunt impedance, Q denotes the quality factor of the resonator and ω_c is its resonant frequency.

If the resonance is sufficiently strong (high Q and large R) the wake field generated by one bunch has a range long enough to affect motion of the neighboring bunches and this may lead to coherent motion of all the bunches. Therefore, for the purpose of our simulation, only the relatively high-Q portion of the longitudinal impedance is relevant. For M equally spaced coupled bunches there are M possible dipole modes labeled by m = 1, 2, ..., M (M coupled oscillators with periodic boundary condition). To illustrate the m-th dipole mode one can look at the θ-position of the centroid of each bunch, θ_ℓ, ℓ = 1, 2, ..., M.

The signature of the simplest coupled bunch mode has the form of a discrete propagating plane wave:

$$\theta_\ell(t) = \theta_o \sin(2\pi m \ell/M - \omega_s t) \ , \qquad (3)$$

where ω_s is the synchrotron frequency.

Based on the analytic model of coupled bunch modes proposed by Krinsky and Wang[4] one can formulate a simple resonant condition for the m-th dipole mode driven by the longitudinal impedance $Z(\omega)$ sharply peaked at ω_c. This condition is given by:

$$\omega_c = (nM + m)\ \omega_o \pm \omega_s \ , \qquad (4)$$

where n is an integer. Since ω_o is time dependent (acceleration) and ω_c is fixed (geometry), and knowing that the width of the impedance peak is governed by ω_c/Q one can clearly see that the resonance condition, Eq. (4), is maintained over a finite time interval. This leads to the useful concept of a mode crossing the impedance resonance. Using the explicit time dependence of ω_o (kinematics) and Eq. (4) one can easily calculate crossing intervals for various modes. This serves as a guide in the simulation since it allows us to select an appropriate time domain where the mode of interest crosses the resonance and will more likely become unstable. The kinematics of the Fermilab Booster can be described as follows:

$$p(t) = (p_o + p^*)/2 - (p^* - p_o)/2 \times \cos 2\pi f t \ , \qquad (5)$$

where

$$f = 15 \text{ Hz}$$

is the frequency of the booster cycle and

$$p_o = 0.650 \text{ GeV/c}$$

$$p^* = 8.889 \text{ GeV/c}$$

are the values of momenta at injection and extraction, respectively.

Now the revolution frequency for the synchronous particle is given explicitly by

$$\omega_o(t) = \frac{c}{R} \left\{ \frac{(pc)^2}{(pc)^2 + (mc^2)^2} \right\}^{1/2}, \qquad (6)$$

where R is the average radius of the ring and p(t) is expressed by Eq. (5). Both Eqs. (5) and (6) allow us to calculate the crossing intervals for different modes. The results are collected in Table 1.

3. UNDAMPED COUPLED BUNCH MODE - ESME SIMULATION

In the early stages of this study we tentatively identified the parasitic resonance at f_c = 167.2 MHz as the offending part of the impedance giving rise to a coupled bunch instability with harmonic number m around 16. More detailed investigation shows (See Table 1) that a sequence of neighboring modes m = 16, 15 and 14 cross the resonance above transition. Due to the fact that the rate of change of the revolution frequency becomes smaller as extraction is approached, the modes passing through the resonance later in the booster cycle stay longer under the driving peak, which suggests that larger integrated growth of these modes might be expected. Therefore we chose to concentrate on the mode with the longest crossing time (m = 14).

f_c [MHz]	R [kΩ]	Q	m	t_o [msec]	t_{cross} [msec]
85.5	914	3378	53	21.80	0.28
109.7	155	2258	7	22.14	0.50
			8	18.18	0.21
225.4	326	2087	23	24.21	0.85
			24	20.98	0.43
			25	19.06	0.28
			26	17.71	0.21
167.2	75.4	1959	14	28.48	1.55
			15	23.11	0.47
			16	21.62	0.27

Table 1. Selected part of the impedance - high Q, large R resonances.[3] Various coupled bunch modes, m, cross these resonances above transition (17.4 - 33. msec). Here t_o denotes the initial time when a given mode matches the frequency at half-maximum of the impedance peak and t_{cross} is the total time necessary for the mode to sweep through the FWHM of the resonance.

The r.f. system of the Fermilab Booster provides 84 accelerating buckets. As a starting point for our simulation each bucket in θ-ε phase-space is populated with 100 macro-particles according to a bi-Gaussian distribution matched to the bucket so that 95% of the beam is confined within the contour of the longitudinal emittance of 0.02 eV×sec. Each macro-particle is assigned an effective charge to simulate a beam intensity of 1.5×10^{12} protons. The appropriate time interval to study mode m = 14 is chosen (according to Table 1) as 26 - 33×10^{-3} sec.

In a real-life accelerator any coherent instability starts out of noise and gradually builds up to large amplitudes. In our model situation it proved necessary to create some intrinsic small amplitude - "seed" of a given mode in order to "start-up" the instability. The "seeding" procedure is basically prescribed by Eq. (3). Initially identical bunches are rigidly displaced from the center of each bucket (both in ε and θ) so that the position of their centroids, θ_l, satisfy Eq. (3) for all the bunches around the ring. In practice, a subroutine of ESME, which generates a closed contour in θ-ε space (given an appropriate starting point) under the action of a sinusoidally varying voltage, was used to establish the position of the bunch centroids. The intrinsic seed amplitude, θ_o, was assigned a value of 10^{-3} rad corresponding to an amplitude in energy of approximately 2 MeV.

The tracking results are illustrated in Fig. 1 by the snapshots of a fraction (one seventh) of the longitudinal phase space taken at initial time, after 2400 revolutions and finally, after 4200 revolutions. Here the initial population was generated according to the above described seeding procedure. One can clearly see development of the m = 14 coupled bunch mode corresponding to increasing amplitude of the dipole oscillations. To visualize the position and shape of individual bunches as they evolve in time one can compose a "mountain range" diagram by plotting θ-projections of the bunch density in equal increments of revolution number and then stacking the projections to imitate the time

flow. The resulting mountain range plot for an undamped mode 14 is given in Fig. 2a.

The same simulation was also repeated for the m = 53 coupled bunch mode, which crosses the f_c = 85.5 MHz parasitic resonance earlier in the booster cycle. According to Table 1, the appropriate time interval to study mode m = 53 is chosen as 19 - 26×10^{-3} sec. Although the crossing time is relatively small (compared to the m = 14 mode) the driving resonance is characterized by the highest Q and largest R. These features distinguish m = 53 as a good candidate for an unstable coupled bunch mode. Indeed, the simulation results illustrated by the mountain range plot, Fig. 3a, and the longitudinal phase-space snapshots collected in Fig. 4 clearly exhibit the signature of a rapidly growing unstable mode (even more pronounced that in the m = 14 case). Extensive filamentation of the bunch edges is also visible in the last snapshot of Fig. 4.

For the remainder of this paper both the m = 14 and m = 53 coupled bunch modes will be studied in a parallel fashion. In the next four sections we will proceed with the discussion of suggested damping mechanisms.

4. FOURTH HARMONIC LANDAU CAVITY - ESME SIMULATION

Now let us consider a situation where, in addition to the fundamental r.f. voltage source, we have a secondary source of voltage whose frequency is equal to that of the fourth harmonic of the fundamental; the so-called Landau cavity. The phase and amplitude of the secondary voltage source are prescribed by the conditions that both the first and second derivatives of the net voltage vanish at the center of each bunch. The above condition can be formulated by introducing both voltages explicitly as follows

$$V_1(\phi) = V_{rf}\ \sin(\phi_s + \phi)$$

and (7)

$$V_4(\phi) = kV_{rf}\ \sin(\phi_4 + 4\phi).$$

Here ϕ_s is the synchronous phase relative to the fundamental r.f. waveform, ϕ_4 is the synchronous phase relative to the fourth harmonic waveform and ϕ denotes the deviation of a particle from the synchronous phase, $\phi = h\theta - \phi_s$. Parameter k is the ratio of the secondary and primary voltage amplitudes. The combined voltage given by:

$$V_{rf}(\phi) = V_1(\phi) + V_4(\phi) \ , \tag{8}$$

is constrained by the following condition:

at $\phi = 0$

$$\text{and} \qquad \begin{aligned} V_{rf}'(\phi) &= 0 \\ V_{rf}''(\phi) &= 0 \ , \end{aligned} \tag{9}$$

which fixes matching parameters k and ϕ_4 as follows

$$\text{and} \qquad \begin{aligned} k &= (1+15\ \cos^2 \phi_s)^{1/2}/16 \\ \phi_4 &= \arccos\ [\ \cos(\pi - \phi_s)/4k]. \end{aligned} \tag{10}$$

The resulting r.f. voltage is illustrated in Fig. 5.

The purpose of imposing the above constraint, Eq. (10), is to provide a highly nonlinear bucket resulting in large synchrotron tune spread within each bunch. This in turn may eventually provide stability against coherent motion of coupled bunches (via a

Landau damping mechanism).

Indeed, by looking at the Hamiltonian for synchrotron oscillation, inside a bucket generated by our modified potential, Eqs. (7)-(10), one can see that instead of a quadratic well the leading term in ϕ has a form of the quartic well;

$$H(p, \phi) = p^2/2 + 5/8 \times \cos(\phi_s)\, V_{rf}\, \phi^4 + O(\phi^5), \qquad (11)$$

where $p = \dot{\phi}$ is the dynamical variable canonically conjugate to ϕ.

Integrating the equations of synchrotron motion generated by the above Hamiltonian one ends up with a ϕ-amplitude dependent synchrotron frequency given by:

$$\omega_s(\phi) = \omega_s{}^o\, (5/2)^{1/2} \times \pi/2 \times \tilde{\phi}/K(1/2)\ . \qquad (12)$$

Here $\tilde{\phi}$ is a peak value of ϕ along a given trajectory and $\omega_s{}^o$ is a synchrotron frequency corresponding to an equivalent harmonic potential and K(x) is the elliptic integral of the first kind.

A family of closed orbits in θ-ε space corresponding to different amplitudes, $\tilde{\phi}$, was generated using a contour drawing subroutine of ESME. The result is depicted in Fig. 6. Each orbit is labeled with the respective synchrotron tune in frequency units (sec^{-1}). The bounding curve, with tune 0, represents the separatrix (note the "squareness" of the bucket in this double r.f. voltage system). Simulated synchrotron tune as a function of amplitude is illustrated in Fig. 7.

The tracking was carried out for exactly the same initial condition as described in the previous section. In addition to the fundamental r.f. voltage the Landau cavity voltage, $V_4(\phi)$, is turned on linearly over the first 2×10^{-3} sec, matched to the fundamental voltage

program according to Eq. (7) for a period of 3×10^{-3} sec and finally turned off linearly over the last 2×10^{-3} sec. The tracking results, as in Sec. 3, are illustrated for both m = 14 and m = 53 coupled bunch modes by the mountain range plots collected in Figs. 2b and 3b. One can see by comparison with the corresponding plots for the undamped mode, Figs. 2a and 3a, that the Landau cavity provides substantial damping of an initially unstable coupled bunch mode (especially for the m = 14 mode).

5. DAMPING THROUGH INTER-BUNCH TUNE SPREAD - ESME SIMULATION

One can apply a secondary voltage source with lower than the fundamental harmonic number. We will consider a situation where 2 out of 18 r.f. cavities, modelled as a secondary source, provide voltage at harmonic number h_2 = 77 (the remaining 16 cavities, modelled as the fundamental r.f. source, will run at h_1 = 84). Now any seven (h_1 - h_2 = 7) consecutive buckets differ due to the voltage modulation provided by the secondary source. Therefore, the value of synchrotron frequency will vary from bunch to bunch (even for small amplitude oscillations in the linear region). For exactly the same initial conditions as in the simulation of the previous section the h_2 = 77 voltage source replaces the Landau cavity with the same linear turn on/off feature.

As before, the phase-space evolution of a single bunch, given by the mountain range plots, Figs. 2c and 3c, illustrate effective damping of m = 14 and m = 53 coupled bunch modes. In fact, in this case the damping is somewhat more evident (especially for m = 53).

The question of relative effectiveness of both cures discussed in Sec. 4 and 5, will be addressed in detail in the next section.

6. INTER- AND INTRA- BUNCH SYNCHROTRON TUNE SPREAD

At this point, some qualitative comments concerning the passive damping mechanisms and their relative efficacy are in order. We note that for mode 53, the cavities operating at harmonic 77 appear to be much more efficient than the Landau cavity (See Figs. 3b and 3c). This is not totally surprising, since the growth of the instability is dependent upon bunch-to-bunch "communication" via wake fields. The $h_2 = 77$ cavities disrupt this communication directly, via bunch-to-bunch tune spread (See Fig. 8). The Landau cavity, on the other hand, operates at an harmonic of the fundamental r.f. frequency, and therefore induces tune spread only within each bunch. The Landau cavity attempts to "discourage" the growth of the instability via suppression of the coherent motion inside each single bunch. The tune spread induced within a bunch, however, is a function of the range of amplitudes of the particles undergoing synchrotron motion (See Fig. 7). Thus, if a group of particles oscillate at amplitude "close" enough to each other, we might expect them to respond to a suitable driving force in a coherent fashion. Presumably, particles may be regarded as "close" if the tune spread among them is smaller than the frequency characterizing the growth of the instability. This "clustering" phenomenon did, in fact, occur in the simulation for mode 53, as illustrated by the mountain range plot in Fig. 3b. It is evident that a cluster of "almost coherent" particles (in the previously described sense) still participates in coupled bunch oscillation, while the remaining particles with synchrotron tune spread larger than some critical value do not respond coherently to the coupling wake field. This would suggest that there exists a threshold tune spread defining the extent of a "coherent blob" inside the bucket; that extent being a characteristic coherence length for a given driving frequency. The same effect is not so evident in the simulation for mode 14. Presumably, the Landau cavity was more effective in this case, because the growth time for this unstable mode is longer. In fact, we

note that the Landau cavity appears to perform better than the $h_2 = 77$ source in this case, which might be due to the apparent increased effectiveness of the Landau cavity as well as the reduced magnitude of the bunch-to-bunch tune spread for the $h_2 = 77$ cavities at later times in the cycle (See Fig. 8).

7. ACTIVE DAMPING THROUGH RADIAL POSITION FEEDBACK - ESME SIMULATION

It was noted that the coupled bunch oscillations in the Fermilab Booster gave rise to a radial position signal in a circuit originally designed to damp horizontal betatron oscillations. It was suggested[6] that this circuit be used to drive a longitudinal broadband kicker, thereby actively damping the coupled bunch modes. This scheme was also simulated. The "kicker" in our simulation delivered a maximum 1kV correction voltage to each bunch; the "seed" amplitude for the mode corresponded to a signal level safely above the noise level of the monitor in the damping circuit, as inferred from observations of the signal and knowledge of the dispersion in the region of the monitor.

Here again the simulation results for both $m = 14$ and $m = 53$ coupled bunch modes are illustrated by the mountain range profiles given in Figs. 2d and 3d. Comparison with the other schemes (See Table 2) indicates that such an active damper is very effective in both cases studied here.

Simulation	$(E - E_o)_{ini}$	$(E - E_o)_{max}$	$(E - E_o)_{fin}$	$(E_{RMS})_{ini}$	$(E_{RMS})_{fin}$
Mode 14:					
a) undamped	1.8	5.2	5.2	3.1	4.7
b) Landau cavity	1.8	1.8	0.1	3.1	2.7
c) $h_2 = 77$ modulation	1.8	1.8	1.2	3.1	2.6
d) active damper	1.8	1.8	0.05	3.1	2.5
Mode 53:					
a) undamped	2.2	6.9	4.1	3.6	5.8
b) Landau cavity	2.2	2.2	1.8	3.6	3.6
c) $h_2 = 77$ modulation	2.2	2.2	0.6	3.6	3.5
d) active damper	2.2	2.2	0.1	3.6	2.9

Table 2. Summary of history plots for various beam parameters recorded during the simulations; E denotes the mean energy of a single bunch, while E_{RMS} is the RMS energy deviation for all the particles around the ring (values are taken on the envelope of the oscillation). Subscripts "ini", "max" and "fin" refer to the initial, maximum and final values of the quantities. All energies are expressed in MeV.

ACKNOWLEDGEMENTS

We wish to thank Chuck Ankenbrandt for encouragement and help, especially in the early stages of this work. We would also like to thank Steve Holmes, Jim Griffin, Bill Ng and others who have contributed many helpful remarks (in the course of numerous meetings addressing the coupled bunch instability problem in the Fermilab Booster). Finally, we wish to thank Peter Lucas, whose work made possible the presentation of the mountain range plots.

REFERENCES

1. J.A. MacLachlan, FERMILAB TM-1274 , 2041.000 (1984)
2. S.A. Bogacz and K-Y. Ng, Phys. Rev. D, **36**, 1538 (1987)
3. J. Crisp, private communication
4. S. Krinsky and J.M. Wang, Particle Accelerators, **17**, 109 (1985)
5. A. Hofmann and S. Myers, CERN ISR-TH-RF/80-26 (1980)
6. C. Ankenbrandt, private communication

FIGURE CAPTIONS

Fig. 1 Time development of the m = 14 coupled bunch mode - θ-ε snapshots taken after various number of turns around the ring.

Fig. 2 Collection of mountain range plots illustrating the behavior of coupled bunch mode m = 14 with:

a) no damping,

b) passive damping via Landau cavity,

c) passive damping through the secondary voltage at h_2 = 77 harmonic,

d) active damping via radial position feedback.

Fig. 3 Collection of mountain range plots illustrating the behavior of coupled bunch mode m = 53 with:

a) no damping,

b) passive damping via Landau cavity,

c) passive damping through the secondary voltage at h_2 = 77 harmonic,

d) active damping via radial position feedback.

Fig. 4 Time development of the m = 53 coupled bunch mode - θ-ε snapshots taken after various number of turns around the ring.

Fig. 5 Combined voltage of a double r.f. system with Landau cavity. The amplitude of the fundamental r.f. component is normalized to unity.

Fig. 6 Synchrotron tune spread inside a highly nonlinear bucket of a double r.f. system with Landau cavity. Simulation corresponds to t =19 msec (Fermilab Booster cycle).

Fig. 7 Synchrotron tune spread inside a bucket corrected by Landau cavity as a function of relative amplitude, $(\varepsilon - E_s)/E_s$, where E_s is the height of the bucket. Discrete markers correspond to the amplitudes and tunes of the orbits collected in Fig. 6.

Fig. 8 Representative bunch-to-bunch tune spread in double r.f. system (for either 1 or 2 of 18 cavities supplying $h_2 = 77$ harmonic modulation). The vertical axis is the difference in the values of the tune (at small amplitude) for the bucket at $\pi/3$ with respect to the modulating voltage and the following bucket.

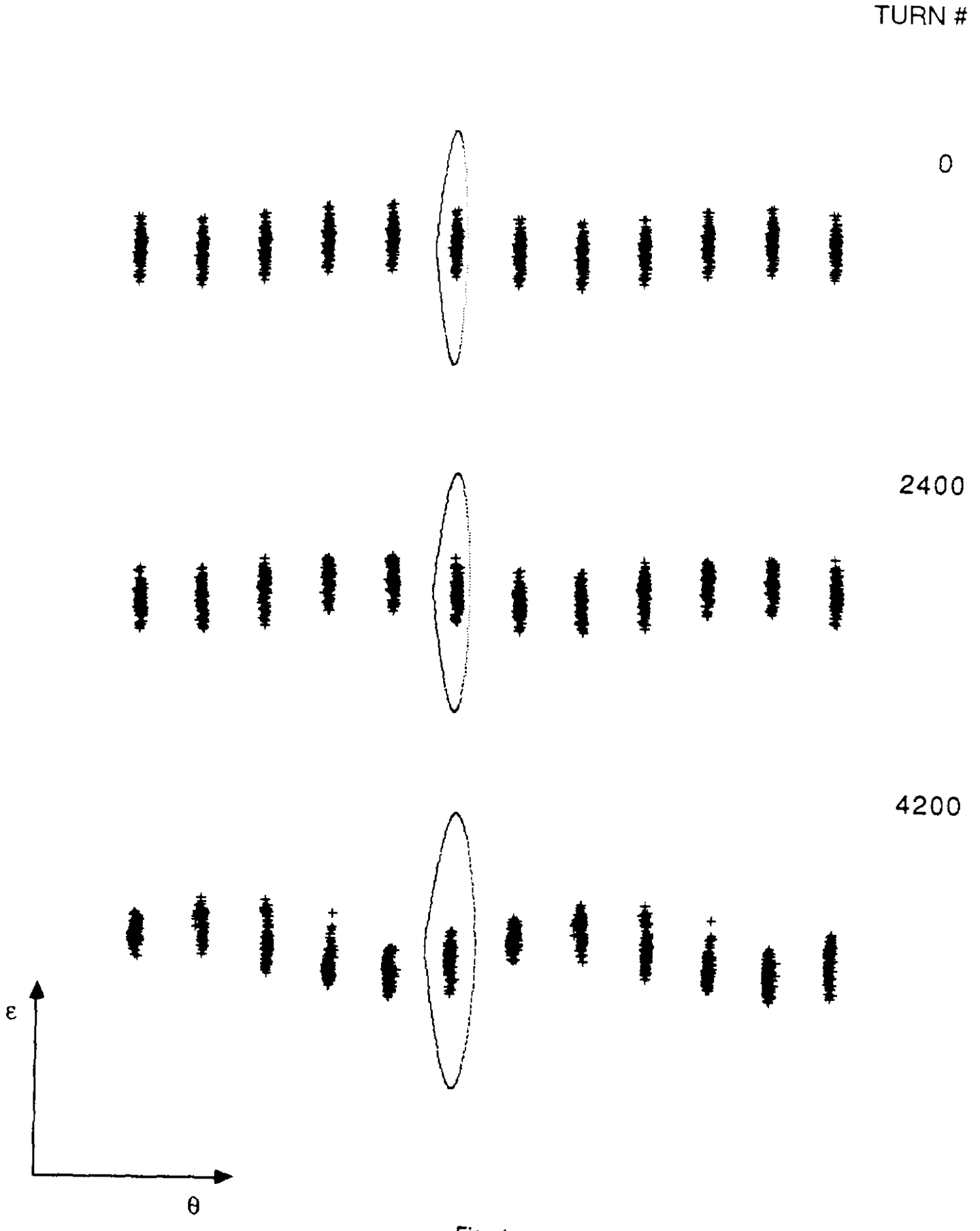

Fig. 1

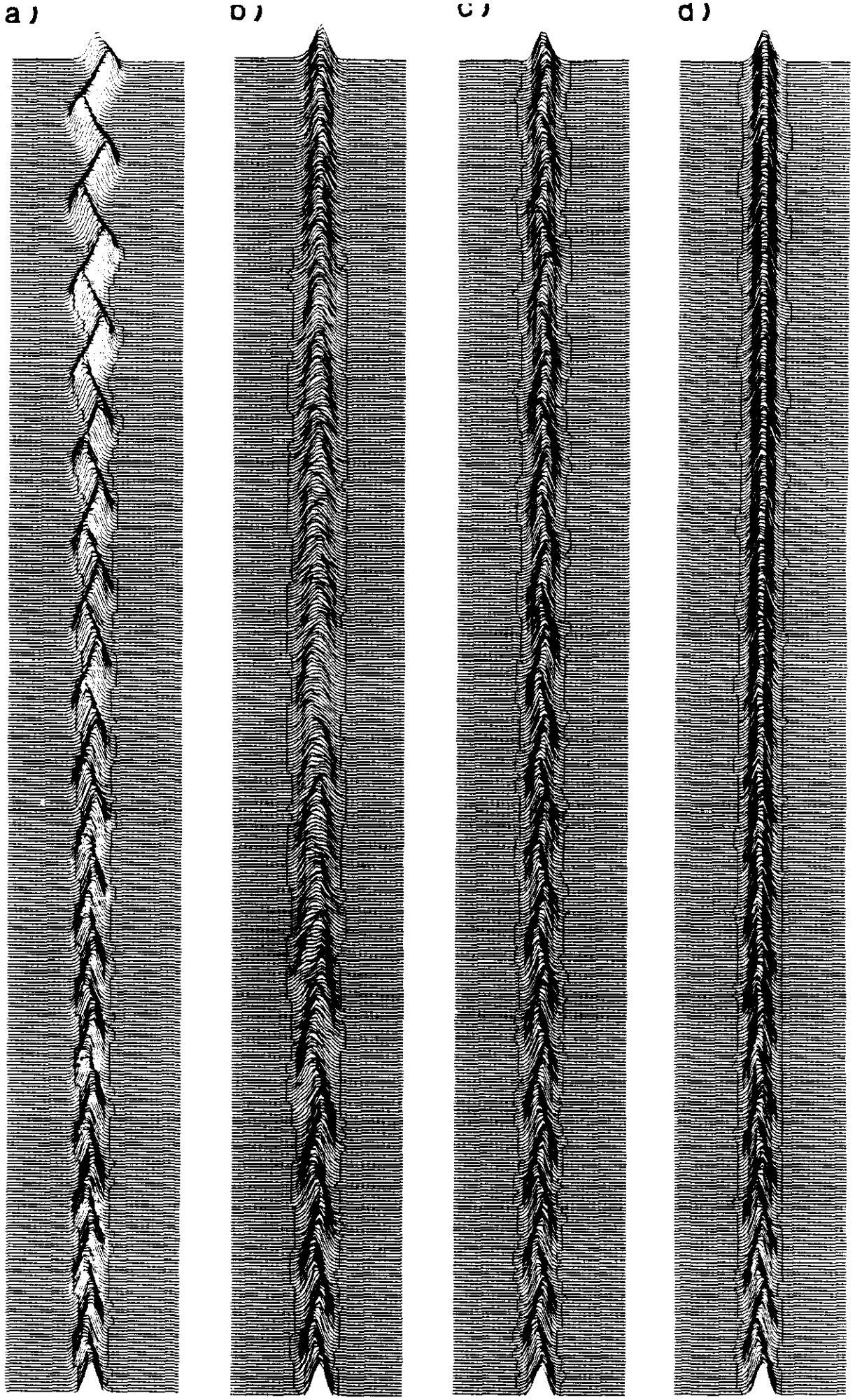

Fig. 2

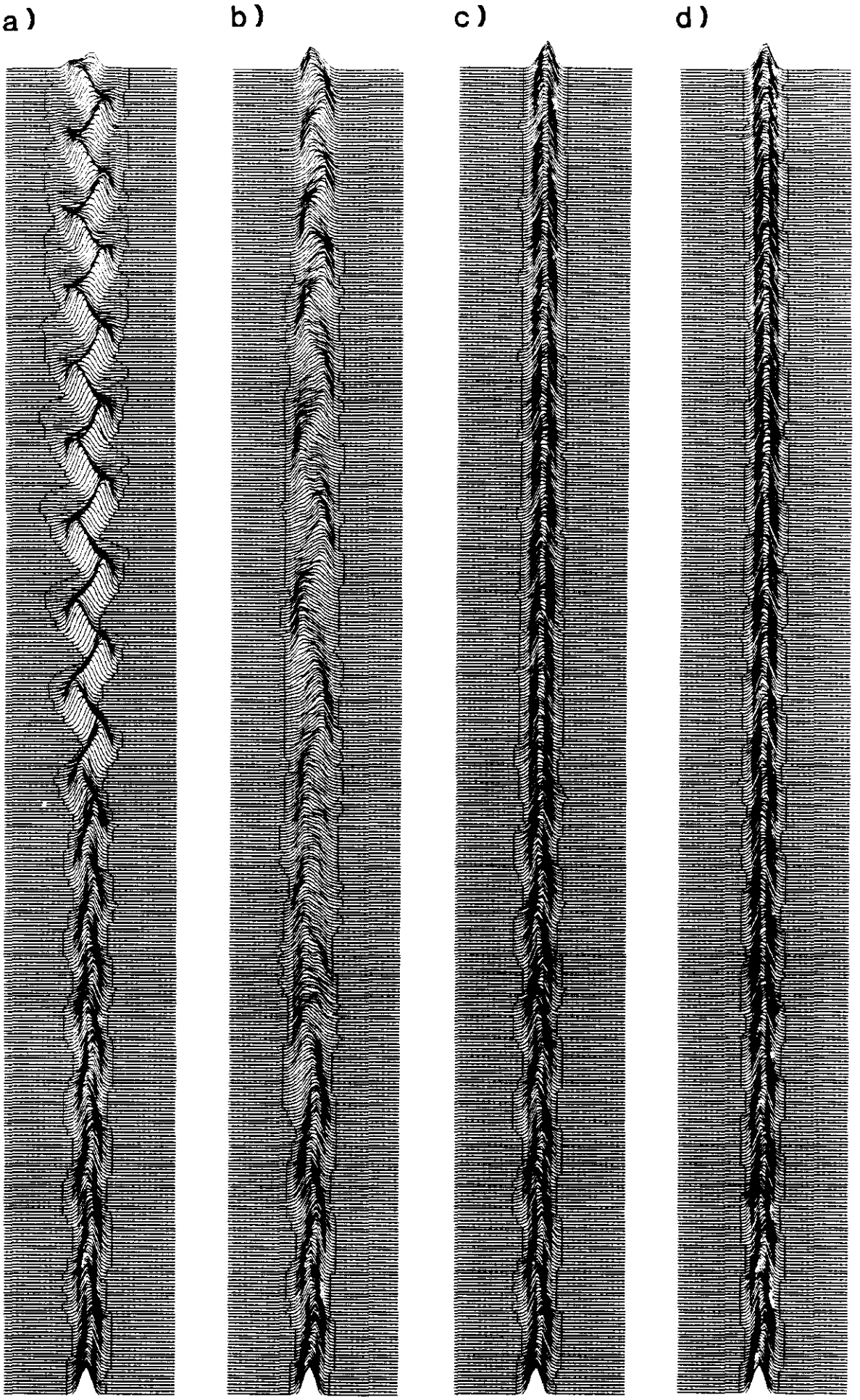

Fig. 3

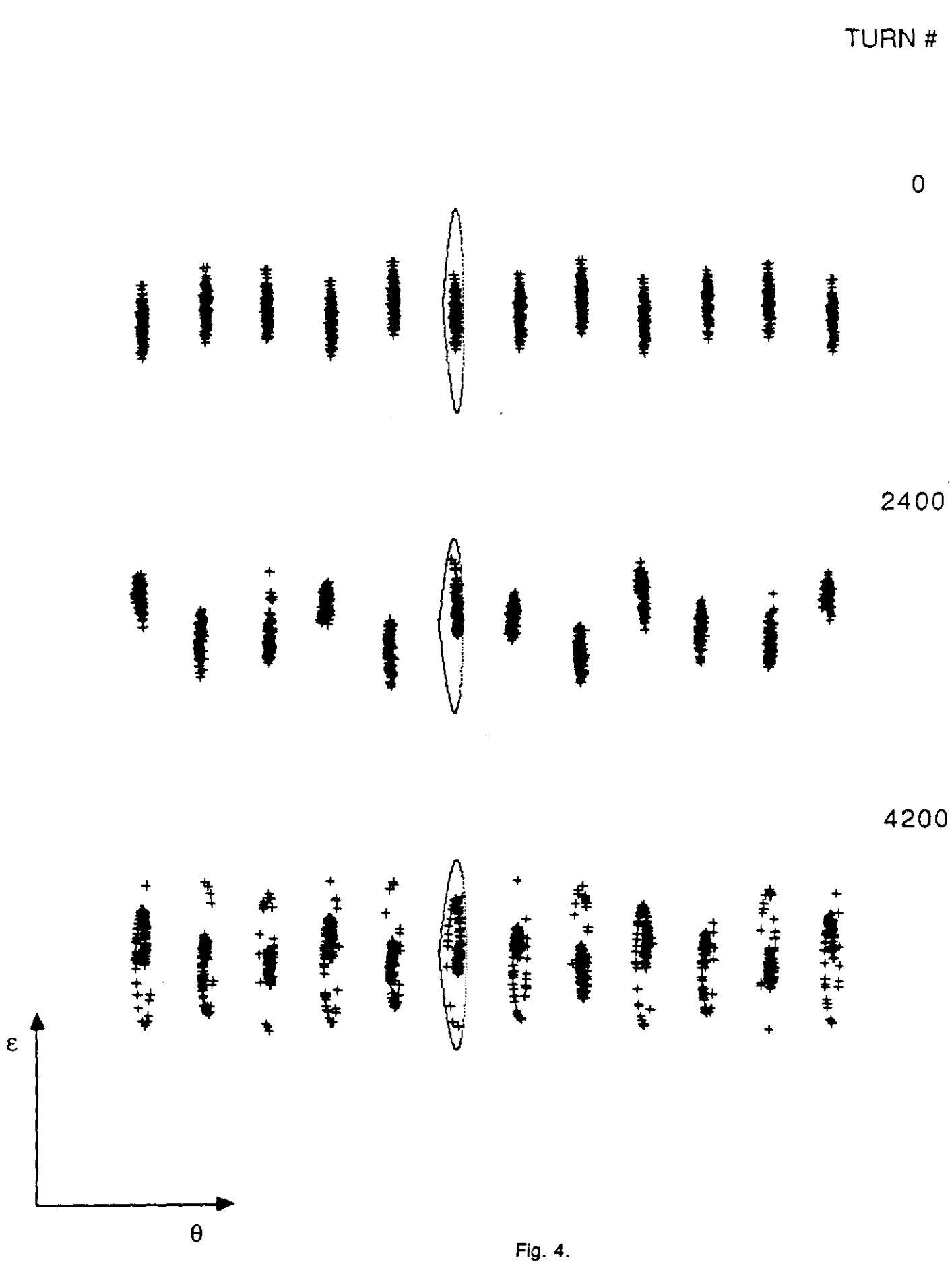

Fig. 4.

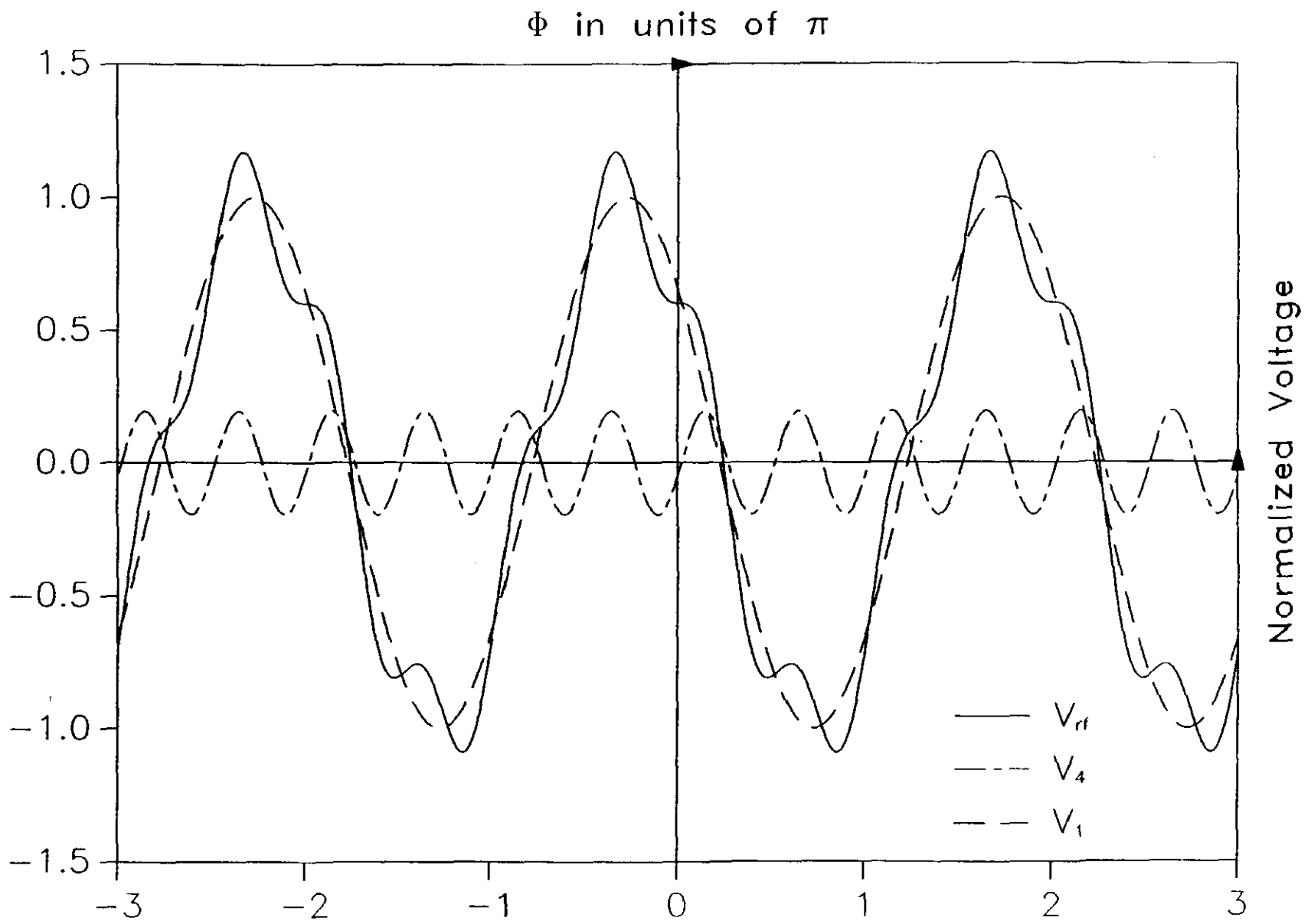
Φ in units of π
1.5
1.0
0.5
0.0
−0.5
−1.0
−1.5
−3
−2
−1
0
1
2
3
Normalized Voltage
V_{rf}
V_4
V_1

Fig. 5

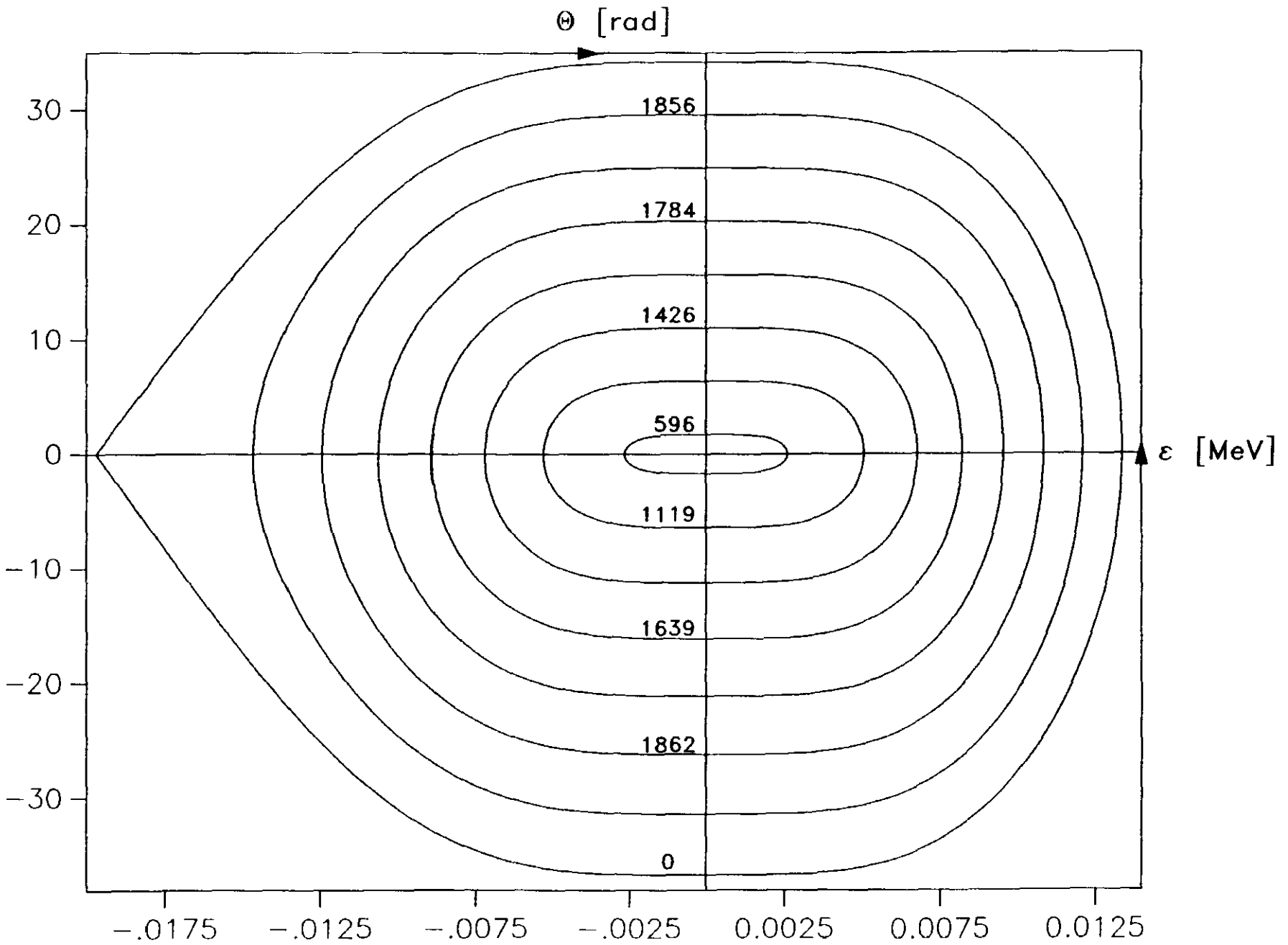
Θ [rad]
30
20
10
0
−10
−20
−30
1856
1784
1426
596
1119
1639
1862
0
ε [MeV]
−.0175
−.0125
−.0075
−.0025
0.0025
0.0075
0.0125

Fig. 6

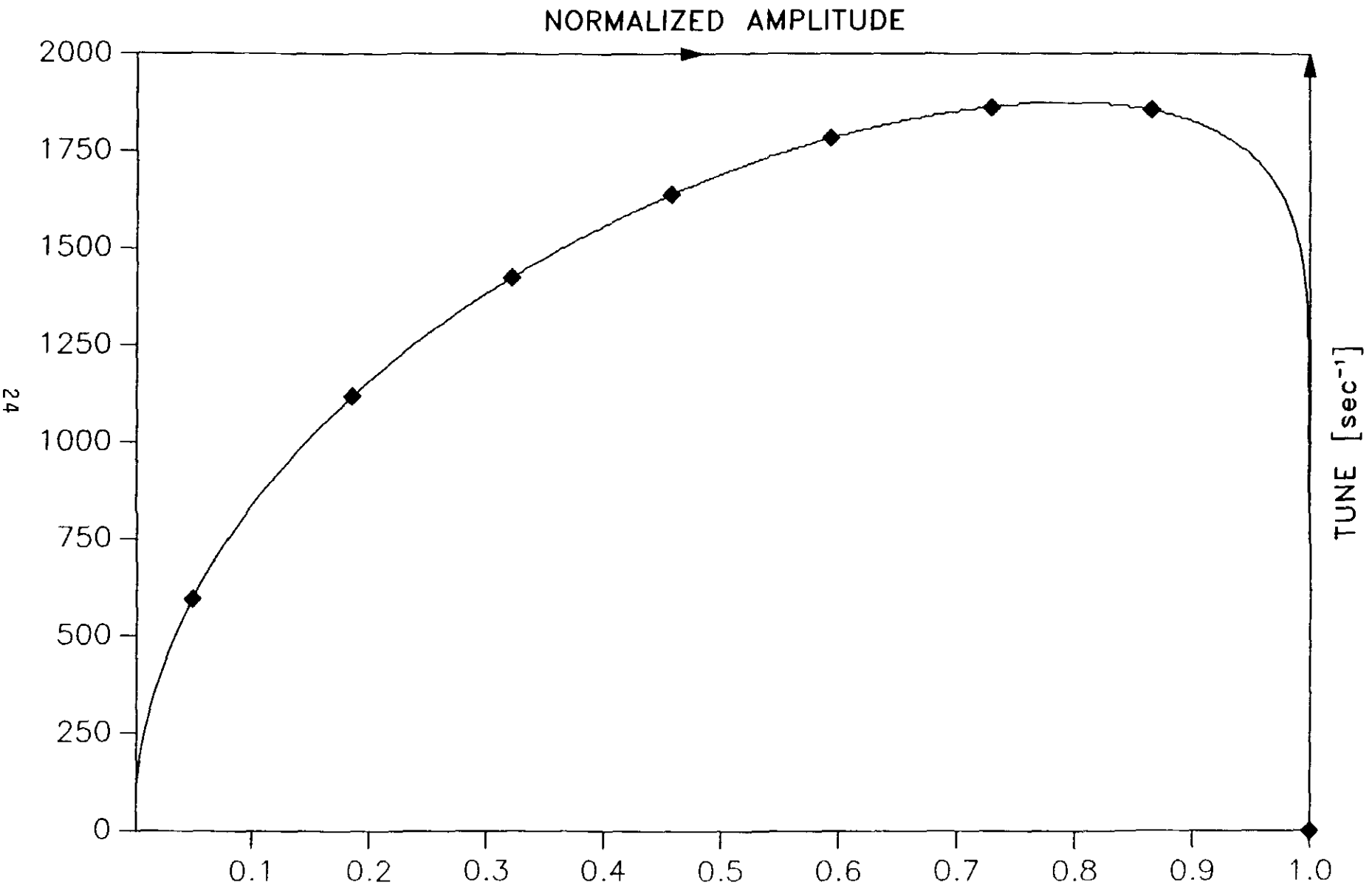
NORMALIZED AMPLITUDE
2000
1750
1500
1250
1000
750
500
250
0
0.1
0.2
0.3
0.4
0.5
0.6
0.7
0.8
0.9
1.0
TUNE [sec⁻¹]

Fig. 7

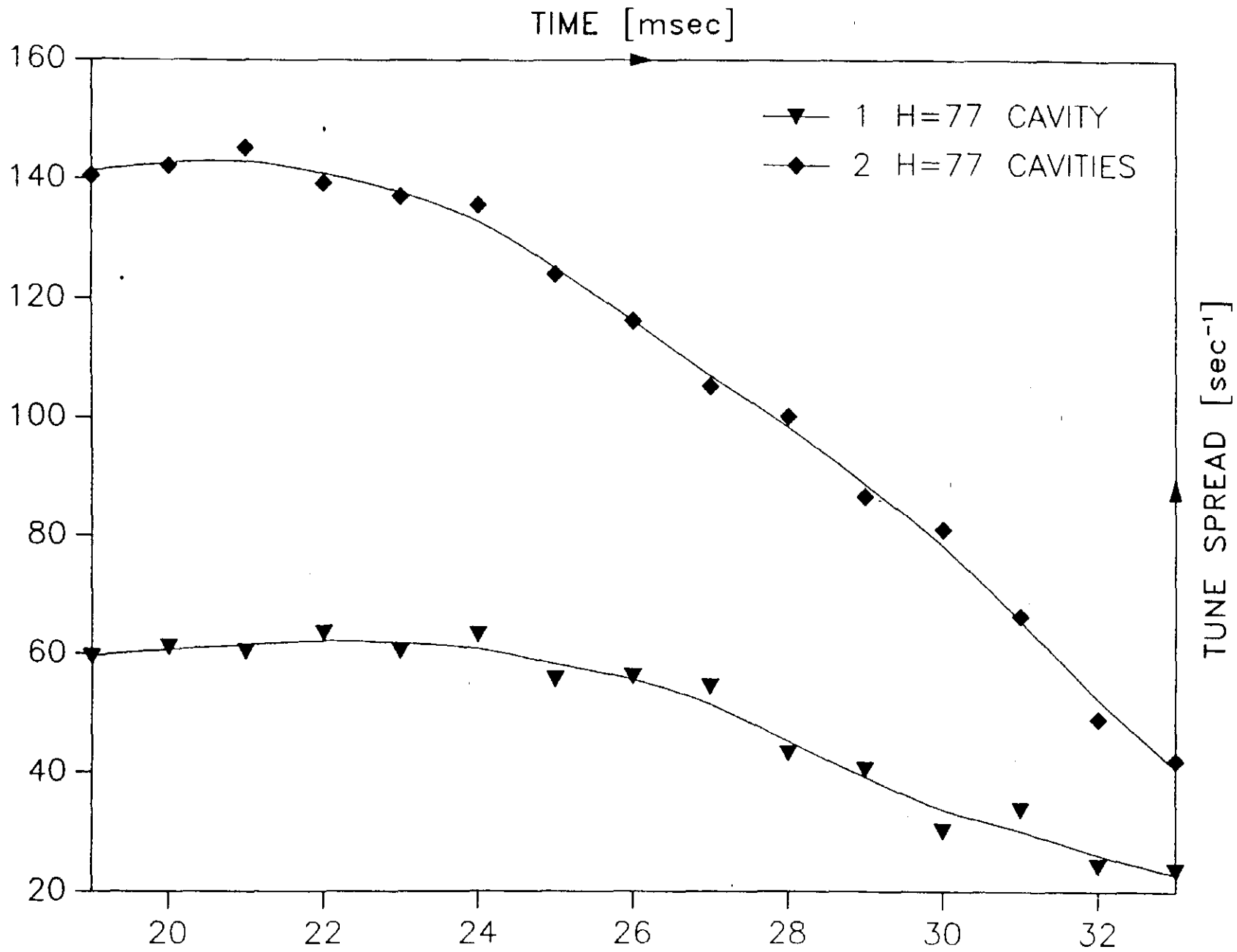
TIME [msec]
160
140
120
100
80
60
40
20
20
22
24
26
28
30
32
1 H=77 CAVITY
2 H=77 CAVITIES
TUNE SPREAD [sec⁻¹]

Fig. 8